

A Systematic Approach to the Optimization of Substrate-Based Inhibitors of the Hepatitis C Virus NS3 Protease: Discovery of Potent and Specific Tripeptide Inhibitors

Montse Llinàs-Brunet,* Murray D. Bailey, Elise Ghiron, Vida Gorys, Ted Halmos, Martin Poirier, Jean Rancourt, and Nathalie Goudreau

Department of Chemistry, Research and Development, Boehringer Ingelheim (Canada) Ltd., 2100 Cunard Street, Laval, Québec, Canada H7S 2G5

Received July 11, 2004

The inadequate efficacy and tolerability of current therapies for the infectious liver disease caused by the hepatitis C virus have warranted significant efforts in the development of new therapeutics. We have previously reported competitive peptide inhibitors of the NS3 serine protease based on the *N*-terminal cleavage products of peptide substrates. A detailed study of the interactions of these substrate-based inhibitors with the different subsites of the serine protease active site led to the discovery of novel residues that increased the affinity of the inhibitors. In this paper, we report the combination of the best binding residues in a tetrapeptide series that resulted in extremely potent inhibitors that bind exquisitely well to this enzyme. A substantial increase in potency was obtained with the simultaneous introduction of a 7-methoxy-2-phenyl-4-quinolinoxy moiety at the γ -position of the P2 proline and a *tert*-leucine as a P3 residue. The increase in potency allowed for the further truncation and led to the identification of tripeptide inhibitors. Structure activity relationship studies on this inhibitor series led to the identification of carbamate-containing tripeptides that are able to inhibit replication of subgenomic HCV RNA in cell culture with potencies below 1 μ M. This inhibitor series has the potential of becoming antiviral agents for the treatment of HCV infections.

Introduction

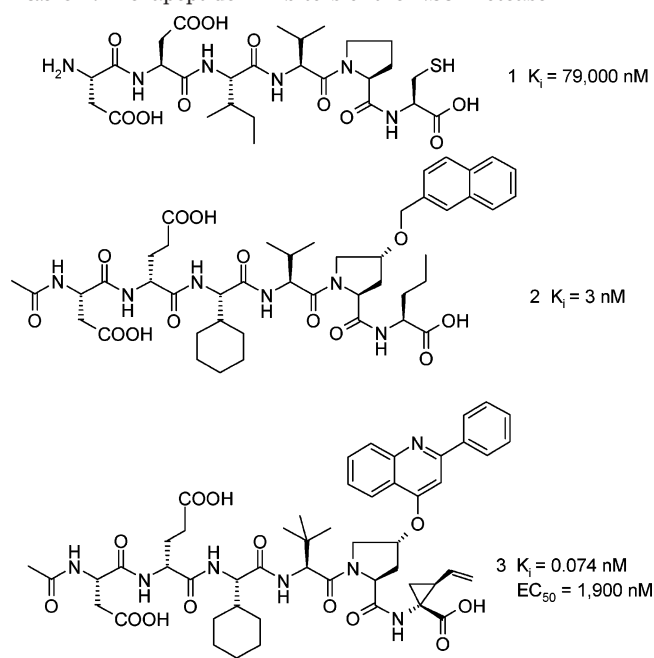
Chronic hepatitis C virus (HCV) infection is a serious cause of liver disease that can lead to cirrhosis and hepatocellular carcinoma in humans.^{1,2} Liver failure due to chronic hepatitis C is now the leading indication for liver transplantation in the developed countries.³ It is estimated that more than 170 million people worldwide are infected with the virus.⁴ Currently, the most effective therapy consists of pegylated α -interferon in combination with the purine nucleoside analogue ribavirin, giving a sustained virological response of \sim 50% in genotype 1 infected patients.⁵ The existing therapies are associated with considerable side effects that lead to discontinuation of treatment in certain patient populations. The limited efficacy and adverse side effects of current therapies, linked to the high prevalence of infection worldwide, clearly highlight the need for more effective, convenient, and well-tolerated treatments. In recent years, a number of reports have appeared describing different classes of compounds targeting key viral enzymes with the expectation that one of these could become the next generation of anti-HCV agents.^{6–8} The first reported compound with proven antiviral activity in a 2-day proof-of-concept in man is BILN 2061, an extremely potent and highly specific NS3 protease inhibitor.^{9,10}

HCV is a small, enveloped virus with a positive-stranded RNA genome which encodes a polyprotein of \sim 3000 amino acids. This polyprotein consists of four

structural and six nonstructural (NS) proteins.¹¹ The structural proteins are processed by host peptidases, whereas the NS proteins are processed by two virally encoded proteases, the NS2/3 and the NS3 proteases. The NS2/3 protease is responsible for the cleavage between NS2 and NS3, while the NS3 protease is responsible for the release of the remaining downstream nonstructural proteins.¹² The NS3 protease, located at the *N*-terminal one-third of the NS3 protein, is a 180 amino acids chymotrypsin-like serine protease.¹³ The function and structure of the NS3 protease have been studied in great detail, making this enzyme perhaps the best understood target of the HCV genome.¹⁴ The essentiality of this enzyme for viral replication has also been demonstrated by the nonproductive infection following liver inoculation of chimpanzees with a genomic HCV RNA mutated in the NS3 protease active site.¹⁵ In addition, the antiviral activity demonstrated by BILN 2061 in the first proof-of-concept in man clearly provided direct validation of the NS3 protease as a valuable target for the development of novel anti-HCV drugs.⁹

We and others have shown that *N*-terminal cleavage products of NS3 protease peptide substrates are competitive inhibitors of this enzyme.^{16,17} This initial finding served as the basis for designing substrate-based inhibitors with hexapeptide DDIVPS–OH (compound **1**, Table 1, $K_{i/app} = 79 \mu$ M) selected as the starting lead.¹⁶ Early optimization led to the identification of norvaline (NVal) as a chemically stable replacement for the P1 cysteine residue.¹⁸ In addition, we discovered that the attachment, through short linkers and with the proper stereochemistry (*R*), of aromatic moieties at the γ

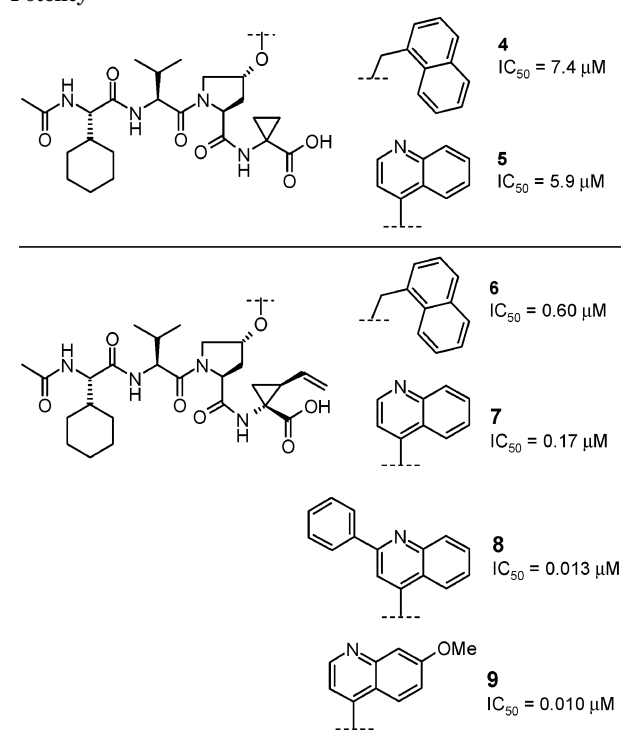
* Corresponding author. Tel: (450) 682-4641 ext-4226. Fax: (450) 682-4189. E-Mail: mllinas@lav.boehringer-ingelheim.com.

Table 1. Hexapeptide Inhibitors of the NS3 Protease

position of the P2 proline moiety provided a significant potency increase (up to 800-fold).¹⁹ Combining these features with optimal substitutions at the P4 and P5 residues led to hexapeptide **2**, a low-nanomolar, competitive inhibitor of the enzyme.¹⁹ Further structure-activity studies culminated in the discovery of a novel P1 residue, (1*R*,2*S*)-1-amino-2-vinylcyclopropanecarboxylic acid (vinyl-ACCA),²⁰ and a more optimized aromatic moiety on the proline,²¹ which altogether gave rise to compound **3**, a picomolar, competitive, and reversible slow-binding inhibitor of the enzyme (Table 1).²² Overall, these studies led to an impressive 10⁶-fold increase in the inhibitory activity. Compound **3** also displayed activity in the cell-based replicon assay,²³ although a large difference between the enzymatic and cell-based potencies (>25 000-fold) was observed, most probably due to the highly peptidic nature of the compound. Since it is well-documented that polypeptides, in particular those containing multiple carboxylate moieties, are unlikely to permeate cells and ultimately to become orally bioavailable,²⁴ we next focused on decreasing the peptidic character as well as the anionic nature of this series of inhibitors.

N-Terminal truncation of different hexapeptides led to the identification of two tetrapeptide inhibitor series represented by compounds **4**¹⁹ and **5**²⁵ (Table 2). Both series displayed similar potency against the enzyme and differed only by the substituent at the 4-*R*-hydroxyproline. Interestingly, these two series became more divergent when combined with our most optimal P1 residue (vinyl-ACCA).²⁰ When vinyl-ACCA was introduced in the more flexible series containing the naphthylmethoxy-substituted P2 proline, a 10-fold increase in potency was observed (**6** vs **4**, Table 2). Surprisingly, the introduction of the optimal P1 residue in the conformationally more constrained inhibitor containing the 4-*R*-quinolinoxy-substituted P2 proline led to a significantly larger improvement in potency (~35-fold, **7** vs **5**).

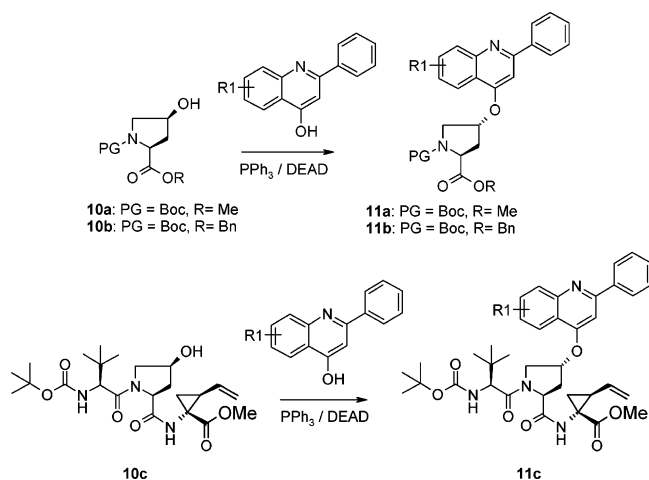
Recently, we also published further improvements on compound **7** through the optimization of the P2 quino-

Table 2. Effect of Combining Optimal Residues on Inhibitor Potency

line moiety. In one study, we showed that the addition of a 2-phenyl ring improved the potency by almost 10-fold, as exemplified by **8**, while in a second study, we showed that the introduction of a 7-methoxy substituent also produced a 10-fold improvement in potency, as demonstrated by **9**.^{21,25} The data shown in Table 2 and in particular the difference in potency between compounds **5** and **9** (>500-fold) highlight the synergistic effect that subtle and beneficial substitutions can have on inhibitor potency. In this paper, we report on our efforts to further improve this series of tetrapeptide inhibitors. Specifically, our goal was to decrease the peptidic nature of these compounds in order to improve their biopharmaceutical properties and thus make this series of inhibitors more “druglike”.

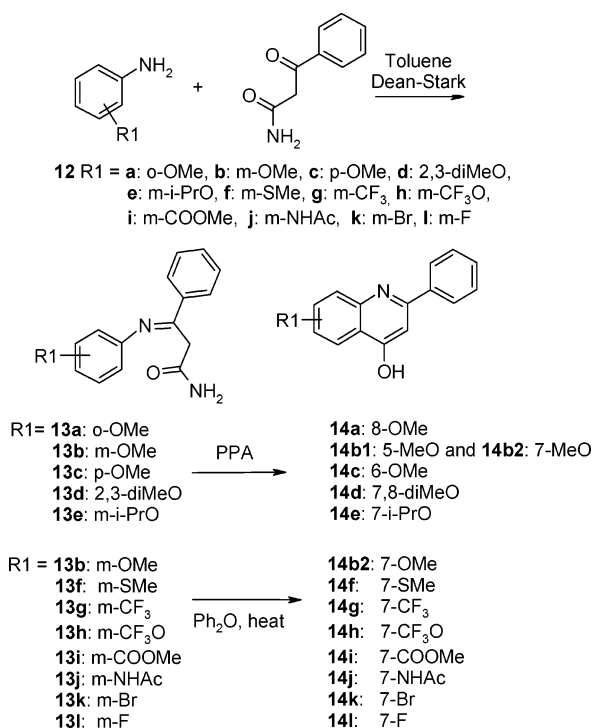
Chemistry

The synthesis of the compounds shown in Tables 3, 4, and 6 was performed in solution by sequential coupling of each amino acid derivative, starting from the *C*-terminal to the *N*-terminal as described previously.^{20,21} The synthesis of (1*R*,2*S*)-1-amino-2-vinylcyclopropanecarboxylic acid methyl ester used in the preparation of these compounds has been reported recently.²⁰ The synthesis of the proline derivatives containing a 4-*R*-aryloxy substituent utilizes either Boc-(4*S*)-*cis*-hydroxyproline methyl (**10a**) or benzyl (**10b**) esters with the introduction of the desired 2-phenylquinolin-4-ol derivative via a Mitsunobu reaction using diethyl azodicarboxylate (DEAD) and triphenylphosphine²⁶ as shown in Scheme 1. The resulting Boc-(4*R*)-aryloxyproline methyl (**11a**) or benzyl (**11b**) ester was hydrolyzed using lithium hydroxide in water/THF to afford the free acid ready for coupling to (1*R*,2*S*)-1-amino-2-vinylcyclopropanecarboxylic acid methyl ester.

Scheme 1. Introduction of Different 2-Phenyl-4-quinolinoxy Substituents on the 4-Hydroxyproline Moiety


For the synthesis of the compounds in Table 5, a more convergent approach was devised. Since these compounds differ only by the nature of their P2 aryloxy substituent, a tripeptide methyl ester intermediate containing the (4*S*)-*cis*-hydroxyproline (**10c**) was first prepared (Scheme 1). The aryloxy moiety was then introduced on tripeptide **10c** via a Mitsunobu reaction using the same diethyl azodicarboxylate (DEAD) and triphenylphosphine reagents²⁶ as above, to yield the desired tripeptide methyl ester **11c**.

The synthesis of the differently substituted 2-phenyl-4-quinolinol derivatives **14** required for the synthesis of the inhibitors was carried out according to the general procedure described by Gardinia *et al.* and is shown in Scheme 2.²⁷ Commercially available, appropriately sub-

Scheme 2. Synthesis of Differently Substituted 2-Phenyl-4-quinolinol


stituted anilines **12** were condensed with 3-oxo-3-phenylpropionyl amide to produce the corresponding imines **13**. Treatment of the imines with either pyrophosphoric acid (PPA) at ~135 °C²⁷ or heating at higher temperatures (250 °C) in diphenyl ether (Ph₂O)^{28,29} produced the appropriately substituted 2-phenylquinolin-4-ol derivatives **14**. Starting with *o*-anisidine (**12a**), the corresponding 8-methoxy-2-phenylquinolin-4-ol (**14a**) was obtained. Similarly, using *p*-anisidine (**12c**) yielded 6-methoxy-2-phenylquinolin-4-ol (**14c**). When 2,3-dimethoxyaniline (**12d**) was used, the required 7,8-dimethoxy-2-phenylquinolin-4-ol (**14d**) was obtained. In the case of *m*-anisidine (**12b**), treatment of its corresponding imine **13b** with PPA resulted in an almost 1:1 mixture of 5- and 7-methoxy-2-phenylquinolin-4-ol (**14b1** and **14b2**, respectively). Both regioisomers could be separated by selective precipitation.²⁷ When the reaction with *m*-anisidine (**12b**) was carried out in diphenyl ether at 250 °C, the 7-methoxy-2-phenylquinolin-4-ol **14b2** was obtained as the major product (11:1). Since the absence of PPA and the higher temperatures favored the formation of the 7-analogue over its 5-substituted counterpart, the synthesis of the 7-substituted-2-phenylquinolin-4-ol derivatives (**14f–14l**) required for the preparation of compounds **27–34** (Table 5) was done by heating the corresponding imines (**13f–13l**) at high temperature in Ph₂O in order to produce almost exclusively the C7-substituted analogues (**14f–14l**).

Results and Discussion

Compound **8** (Table 3) was selected as the starting point for further optimization. As previously observed for hexapeptide inhibitors,^{16,19} tetrapeptide **8** was shown to be a competitive inhibitor of the enzyme with a *K*_i of 6 nM. In addition, compound **8** was found to be very specific for the HCV NS3 protease and did not inhibit other serine/cysteine proteases such as human leukocyte elastase or cathepsin B (IC₅₀ > 30 μM).

A model of inhibitor **8** bound to the active site of the NS3 protease was also generated. Recently, we have published the NMR-derived bound conformation of a tripeptide analogue of **8**, along with its complex model to the NS3 protease.²¹ This model showed the inhibitor bound in an overall extended conformation, similar to that of other previously studied inhibitors.^{30–34} Using this complex model as a guide²¹ along with the published crystal structure of the full length NS3 protein,³⁵ compound **8** was docked and minimized into the active site of the NS3 protease to generate the model shown in Figure 1. In this complex model, the P1, P2, P3 residues, as well as the C-terminal carboxylic acid of **8**, make very similar interactions with the enzyme to those reported previously for related analogues.^{21,36} In addition, the carbonyl of the acetyl capping group is involved in a hydrogen bond with the backbone NH moiety of Cys159, while the P4 cyclohexylglycine moiety occupies the shallow S4 binding pocket of the enzyme formed by residue Val158 and in part by the side chains of Arg123, Ala156, and Asp168.

Compared to other chymotrypsin-like serine proteases, the NS3 protease lacks several surface loops

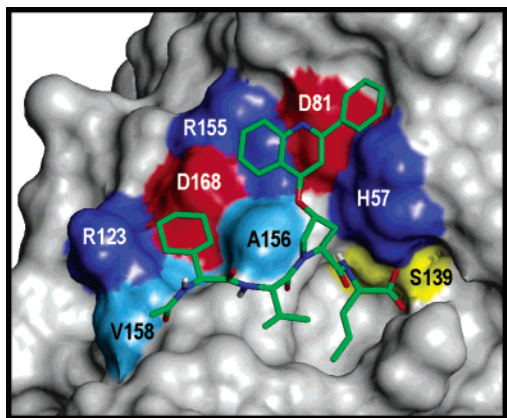


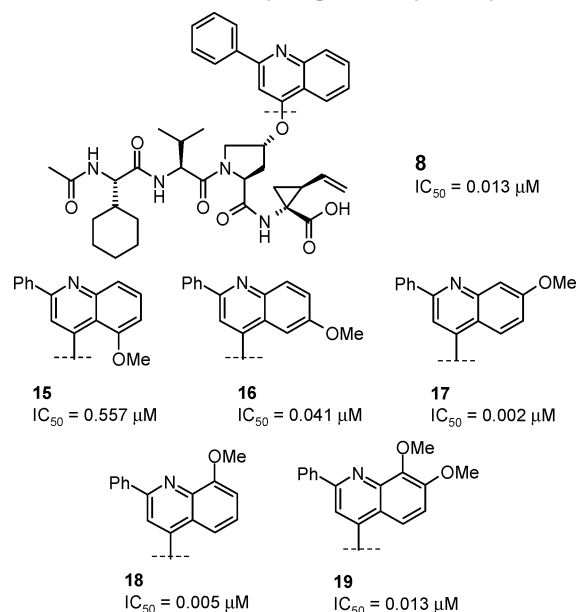
Figure 1. Model of inhibitor **8** bound into the active site of the NS3 protease–NS4A complex. In this model, the NS3 is represented as a Connolly surface, while the inhibitor is represented in sticks and is colored by atom type. For clarity, most of the hydrogen atoms are omitted.

usually located around the S2 and S4 subsites, resulting in a shallower and more solvent-exposed binding cleft.³⁷ The NS3 protease S2–S4 binding region (at least for genotypes 1 and 2) is rather unique, in that it is constituted by a stretch of residues with alternating positively and negatively charged side chains. Starting with the catalytic His57 and Asp81 moieties and following with Arg155, Asp168, and Arg123, this stretch of alternating charged residues can interact and neutralize each other through various intramolecular hydrogen bonding and/or electrostatic interactions (Figure 1). Previous SAR studies published by us^{19,21,22,25} and others^{38,39} have highlighted the beneficial effect of large hydrophobic residues at the P2 and P4 positions on inhibitor binding. From the complex model, we can see that these particular residues lie on the enzyme surface and partially shield the stretch of charged residues from solvent. It is assumed that this shielding effect somehow stabilizes the protein by increasing the strength of the intramolecular hydrogen bond and/or electrostatic interactions.^{21,33} These observations therefore prompted us to further investigate SAR at the P2 and P4 positions of our tetrapeptide inhibitor series.

We have previously shown that the addition of a methoxy group at the C7-position of the 4-quinolinoxy moiety of the tetrapeptide inhibitors provided a 10-fold increase in their potencies (See **9** vs **7**, Table 2).^{20,25} The effect of the systematic introduction of a methoxy group at the different positions of the quinoline ring B in a more optimal series of inhibitors containing the 2-phenylquinolin-4-ol moiety was evaluated. This study was performed on compound **8**, and results are summarized in Table 3. Introduction of a methoxy group at the C5-position of the quinoline moiety was highly detrimental to potency, as seen with tetrapeptide **15**. This significant loss in potency might be due to an unfavorable interaction between the C5-methoxy group and the rest of the inhibitor, which would destabilize the bioactive conformation, or to a steric clash between the C5-methoxy group and the enzyme side chain of Ala156. Introduction of a C6-methoxy, as in compound **16**, was tolerated, resulting in a 2-fold loss in potency. Interestingly, the

introduction of either a C7- or C8-methoxy substituent showed an approximate 5-fold increase in the potency of the corresponding inhibitors (compounds **17** and **18**), giving rise to the first tetrapeptide inhibitors displaying IC_{50} below 10 nM in the *in vitro* enzymatic assay. We believe that this increase in potency might be attributed to a favorable interaction between the guanidine moiety of the protease Arg155 side chain and the C7- or C8-methoxy quinoline unit. In fact, such an interaction was observed in the recently reported X-ray crystal structure of a macrocyclic analogue of **17** bound to the active site of the NS3 protease–NS4A complex.³⁶ Finally, since both the introduction of a C7- and a C8-methoxy produced a significant increase in potency, the corresponding C7,C8-disubstituted analogue **19** was prepared. Disappointingly, disubstitution did not produce the desired additive effect, and **19** was found to be less potent than the individual monosubstituted inhibitors (**17** and **18**). Overall this study highlighted that in this series of inhibitors containing the 2-phenylquinoline moiety, the introduction of a 7- or a 8-methoxy group was beneficial for potency. Compound **17** was used for subsequent optimization.

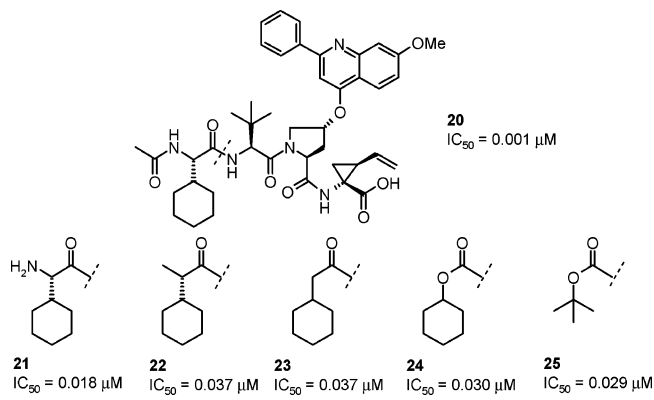
Table 3. SAR on the 2-Phenyl-4-quinolinoxy Moiety



Previous structural studies indicated that both the NH and CO groups of the P3 residue are involved in hydrogen bonding to the protein backbone and that the major role of the P3 side chain is to rigidify and predefine the overall extended conformation in the free-state to resemble the bound one.^{21,36,40} On this basis, we envisioned that a bulkier side chain than that of valine should be well-tolerated at P3. Compound **20** (Table 4) containing a *tert*-leucine residue turned out to be also a very potent inhibitor of the NS3 protease. Encouraged by these results, we decided to reduce the peptidic nature by performing a systematic *N*-terminal truncation study. These results are shown in Table 4. Removal of the acetyl capping group produced the amino-terminal tetrapeptide **21**, which displayed a large

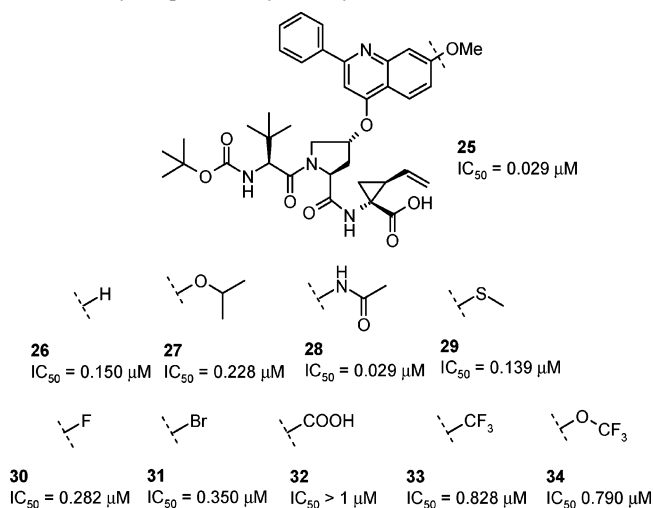
decrease in potency (~ 20 -fold). This loss in binding affinity is consistent with our complex model (Figure 1), which highlights the involvement of the acetyl carbonyl moiety in a hydrogen bond to the backbone of the NS3 protease (NH of Cys159). Replacement of the amino group by a methyl group, as in **22**, or by a simple hydrogen atom, as in **23**, was well-tolerated, producing only a small decrease in potency. Interestingly, when the C2-methylene unit of **23** was replaced by an oxygen atom, to yield the corresponding carbamate **24**, the binding affinity of the inhibitor was maintained. In addition, the cyclohexyl could also be replaced by a *tert*-butyl group to produce carbamate **25**, a potent tripeptide inhibitor of the NS3 protease. Finally, these tripeptide inhibitors also maintained their specificity against other serine proteases, as shown by the lack of inhibitory activity of compound **25** when tested against the human leucocyte elastase ($IC_{50} > 75 \mu M$).

Table 4. Systematic *N*-Terminal Truncation



After establishing the tripeptide inhibitor series, we evaluated the requirements of the C7-substituent of the 2-phenylquinolin-4-oxy moiety, to see if other groups would offer an advantage over the methoxy. This study was conducted on analogue **25**, and the results are shown in Table 5. A variety of groups differing in size and electronic properties were evaluated. As expected, removal of the methoxy group produced a loss in activity, as seen with **26**. Replacement of the methoxy moiety by an acetyl amino group, as in **28**, was well-tolerated, producing an equipotent inhibitor. Increasing the size of the alkoxy moiety to an isopropoxide as in **27** or replacing it by a thiomethyl as in **29** was detrimental in both cases, producing a 5–6-fold decrease in potency. The loss in potency was even more substantial when a C7-halogen (F, Br) was introduced as in **30** and **31**. Finally, the largest decrease in potency was observed when electron-withdrawing groups such as a $-CF_3$ (compound **33**); $-OCF_3$ (compound **34**), and $-COOH$ (compound **32**) were introduced at this position. In summary, from all the different groups evaluated at the C-7 position of the 2-phenylquinolin-4-oxy moiety in this study, the methoxy was found to be the most beneficial one. This preference is not fully understood at this point and most probably results from a subtle balance between the hydrophobicity, bulkiness, electronic properties, and polarizability of this substituent.

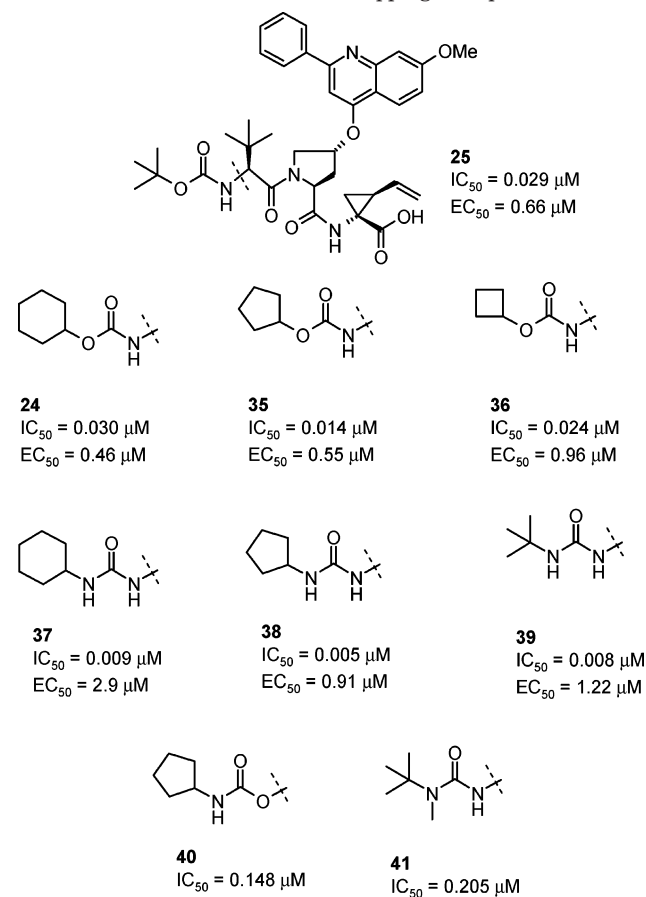
Table 5. Evaluation of Different Groups at the 7-Position of the 2-Phenyl-4-quinolinoxyl Moiety



The next step focused on the optimization of the capping group. Tripeptide **25**, containing a *tert*-butyl carbamate, is a potent inhibitor of the HCV NS3 protease. Interestingly, the interaction between a *tert*-butyl carbamate capping group and the S4 binding pocket of the enzyme was previously observed in the X-ray crystal structure of a macrocyclic analogue of **25** bound to the NS3 protease.³⁶ Specifically from this X-ray cocomplex structure it can be seen that the carbamate functionality effectively positions the *tert*-butyl group in the shallow S4 binding pocket of the enzyme, composed of residue Val158 and in part by the side chains of Arg123, Ala156, and Asp168. In addition, when compound **25** was evaluated in the cell-based replicon assay,²³ we were quite pleased to see that it displayed a submicromolar potency (EC_{50} of 660 nM), making this series of tripeptide inhibitors interesting candidates for further optimization. Carbamates arising from cyclic alcohols (Table 6) were chemically more stable than the *tert*-butyl carbamate and produced potent analogues, such as the cyclobutyl (**36**), the cyclopentyl (**35**), and the cyclohexyl (**24**) derivatives. The cyclopentyl derivative **35** proved to be the most potent analogue of this series, showing a 2-fold increase in enzymatic potency, which unfortunately was not reflected in the cellular assay. To further explore the SAR of the capping group, several approaches were attempted. First, the corresponding urea derivatives of carbamates **24**, **35**, and **36** were prepared. As shown in Table 6, replacement of the carbamate moieties by their urea counterparts led to a 3–4-fold improvement in the enzymatic potency of the new inhibitors, as exemplified by **37**, **38**, and **39**. Unfortunately, this increase in potency did not translate into the cell-based assay, with the urea derivatives being 2–5-fold less potent than the corresponding carbamates. The second approach consisted of introducing a reverse carbamate moiety. Compound **40**, containing a reverse carbamate at the *N*-terminus, was found to be significantly less potent than its corresponding carbamate analogue **25**. The last modification was the *N*-alkylation of the urea derivative **39**, which led to compound **41** and resulted again in a significant loss in potency. In summary from all these results, compound **35** proved

to be our best overall inhibitor with good potencies in both the enzymatic and cell-based assays.

Table 6. Evaluation of Different Capping Groups



To provide an explanation as to why inhibitors containing an *N*-terminal urea moiety bind more efficiently to the enzyme than the corresponding carbamate analogues, we generated a model of inhibitor **38** bound to the active site of the NS3 protease–NS4A_{peptide} complex, as shown in Figure 2. In general, for most peptidic inhibitors of chymotrypsin/trypsin-like serine proteases, the P3 residue is involved in intermolecular antiparallel β -sheetlike interactions with one of the enzyme residues. Specifically for the NS3 protease, it has been observed that both the CO and NH moieties of the P3 residue are involved in hydrogen bonds with the NH and CO of Ala157, respectively.^{21,33–36} In the case of derivative **38**, we can observe in our model that both NH moieties of the urea are capable of forming a hydrogen bond with the main chain carbonyl of Ala157, as shown in Figure 2. This urea–carbonyl bidentate interaction could explain the consistent 3–4-fold increase in potency observed for the urea derivatives over their carbamate counterparts. In addition, it also provides an explanation as to why compound **41**, containing an *N*-methylurea directly pointing at the enzyme, was significantly less potent. Interestingly, this particular type of bidentate interaction has also been observed recently for another substrate-based NS3 protease inhibitor containing a similar urea capping group.⁴¹ The other interactions between inhibitor **38** and the enzyme were found to be very similar to the ones reported previously for related analogues containing *C*-terminal

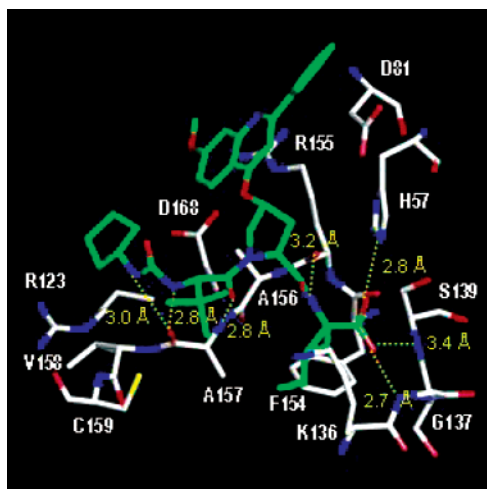


Figure 2. Model of inhibitor **38** bound into the active site of the NS3 protease–NS4A complex. Key hydrogen bond interactions between **38** and the NS3 protease are represented by dashed yellow lines. For clarity, hydrogen atoms are omitted.

carboxylic acid, in particular, for a tripeptide macrocyclic inhibitor for which we also obtained an X-ray crystal structure in complex to the NS3 protease.³⁶ Finally from Figure 2, we can also see that the cyclopentyl moiety of the urea capping group is properly positioned in the S4 binding pocket of the enzyme, thus providing additional interactions.

Conclusion

Inhibitors of the HCV NS3 serine protease based on *N*-terminal cleavage products of peptide substrates have the potential to become efficacious antiviral agents for the treatment of chronic HCV infections. The first compound reported to have an antiviral activity in a proof-of-concept in humans, BILN 2061, was derived from this class of inhibitors.⁹ Starting from *N*-terminal substrate-based tetrapeptide inhibitors, the P1 residue and the aromatic substituent at the γ -position of the P2 proline were quickly identified as the major contributors to the potency of these compounds. Further optimization of the P2 proline aromatic moiety resulted in the identification of 7-methoxy-2-phenylquinolin-4-oxy as the best substituent to provide good potency in the enzymatic assay. The introduction of this particular moiety in our tetrapeptide lead series resulted in very potent inhibitors with low nanomolar IC_{50} 's. The peptidic nature of these compounds was then reduced by conducting a systematic *N*-terminal truncation study. This work allowed for the identification of new potent tripeptide inhibitors containing either a carbamate or a urea capping group. We believe that the somewhat rigid nature of these functionalities allows for the proper positioning of the *N*-terminal alkyl group into the S4 binding pocket of the enzyme. The *N*-terminal urea inhibitor series benefits from an additional hydrogen-bond interaction with the enzyme, compared to the carbamate analogues, resulting in an increase of their inhibitory activities. In summary, tripeptide inhibitors of the NS3 protease displaying low nanomolar and submicromolar potencies in the enzymatic and the cell-based replicon assays respectively have been identified in this work. Studies are underway to further improve

the potency and reduce the EC₅₀/IC₅₀ ratio of this new promising tripeptide inhibitor series.

Experimental Section

Materials. The synthesis of (1*R*,2*S*)-1-amino-2-vinylcyclopropanecarboxylic acid methyl ester used in the preparation of these compounds has been recently described.²⁰ The synthesis of the 5- and 7-methoxy-2-phenylquinolin-4-ol (**14b1** and **14b2**) was carried out according to the published protocol.²⁷

Preparation of 2-Phenylquinolin-4-ol Derivatives 14a and 14c–14e. The same general procedure described for the preparation of the **14b1** and **14b2** derivatives²⁷ was used for the synthesis of the 8-methoxy (**14a**), 6-methoxy (**14c**), 7,8-dimethoxy (**14d**), and 7-isopropoxy-2-phenylquinolin-4-ol (**14e**) derivatives.

A solution containing 3-oxo-3-phenylpropionamide (2 mmol), aniline derivative (2.1 mmol), and the hydrochloride salt of the aniline derivative (0.15 mmol) in toluene (10 mL) was refluxed in a Dean–Stark apparatus for 6–8 h. The solution was cooled to room temperature and concentrated. Flash column chromatography using a mixture of hexanes and ethyl acetate afforded the desired imine **13a** and **13c–13e** in 85–90% yield. A mixture of the required imine and pyrophosphoric acid (PPA) (10-fold w/w) was then heated at 135 °C for ~1 h. Water was added and the solution was rendered to pH 8 by adding 20% aqueous NaOH. After stirring for 15 min the desired 4-quinolinol derivatives precipitated and were collected by filtration.

8-Methoxy-2-phenylquinolin-4-ol (14a): Starting with *o*-anisidine (**12a**) the title compound was obtained in 18% yield. ¹H NMR (DMSO-*d*₆): δ 10.71 (br s, 1H), 7.79–7.71 (m, 2H), 7.68–7.64 (m, 1H), 7.57–7.51 (m, 3H), 7.31–7.24 (m, 2H), 6.28 (br s, 1H), 3.97 (s, 3H).

6-Methoxy-2-phenylquinolin-4-ol (14c): Starting with *p*-anisidine (**12c**) the title compound was obtained in 39% yield. ¹H NMR (DMSO-*d*₆): δ 7.85–7.81 (m, 2H), 7.72 (d, *J* = 8.9 Hz, 1H), 7.60–7.54 (m, 3H), 7.50 (d, *J* = 2.9 Hz, 1H), 7.31 (dd, *J* = 3.0, *J'* = 8.9 Hz, 1H), 6.35 (br s, 1H), 3.84 (s, 3H).

7,8-Dimethoxy-2-phenylquinolin-4-ol (14d): Starting with 2,3-dimethoxyaniline (**12d**) the title compound was obtained in 12% yield. ¹H NMR (CDCl₃): δ 8.78 (br s, 1H), 8.09 (d, *J* = 8.9 Hz, 1H), 7.70–7.66 (m, 2H), 7.57–7.52 (m, 3H), 7.04 (d, *J* = 8.9 Hz, 1H), 6.53 (s, 1H), 4.06 (s, 3H), 4.01 (s, 3H).

7-Isopropoxy-2-phenylquinolin-4-ol (14e): Starting with *m*-isopropoxyaniline (**12e**) the title compound was obtained in 21% yield. ¹H NMR (CDCl₃): δ 8.07 (d, *J* = 9.2 Hz, 1H), 7.70–7.64 (m, 2H), 7.40 (d, *J* = 1.9 Hz, 1H), 7.35–7.29 (m, 3H), 6.80 (dd, *J* = 2.3, *J'* = 8.9 Hz, 1H), 6.22 (s, 1H), 4.54–4.46 (m, 1H), 1.24 (d, *J* = 6.1 Hz, 6H).

Preparation of 7-Substitued-2-phenylquinolin-4-ol Derivatives 14f–14k.

A solution containing 3-oxo-3-phenylpropionamide (2 mmol), aniline derivative **12f–12l** (2.1 mmol), and the hydrochloride salt of the aniline derivative (0.15 mmol) in toluene (10 mL) was refluxed in a Dean–Stark apparatus for 6–8 h. The solution was cooled to room temperature and concentrated. Flash column chromatography using a mixture of hexanes and ethyl acetate afforded imines **13f–13l** (85–90% yield). A mixture of the desired imine and diphenyl ether (5 mL) was then heated at 240 °C for ~1 h. The solution was cooled to room temperature and dichloromethane was added. The solid was collected by filtration.

7-Methoxythio-2-phenylquinolin-4-ol (14f): Starting with *m*-methylthioaniline (**12f**) the title compound was obtained in 21% yield. ¹H NMR (DMSO-*d*₆): δ 7.97 (d, *J* = 8.6 Hz, 1H), 7.84–7.79 (m, 2H), 7.61–7.54 (m, 4H), 7.19 (dd, *J* = 1.7, *J'* = 8.4 Hz, 1H), 6.29 (s, 1H), 2.56 (s, 3H).

2-Phenyl-7-(trifluoromethyl)quinolin-4-ol (14g): Starting with *m*-trifluoromethylaniline (**12g**) the title compound was obtained in 33% yield. ¹H NMR (DMSO-*d*₆): δ 8.29 (d, *J* = 7.9 Hz, 1H), 8.15 (br s, 1H), 7.91–7.83 (m, 2H), 7.66–7.58 (m, 4H), 6.47 (s, 1H).

2-Phenyl-7-(thrifluoromethoxy)quinolin-4-ol (14h): Starting with *m*-trifluoromethoxyaniline (**12h**) the title com-

ound was obtained in 31% yield. ¹H NMR (DMSO-*d*₆): δ 8.20 (d, *J* = 8.9 Hz, 1H), 7.87–7.82 (m, 2H), 7.72 (br s, 1H), 7.62–7.56 (m, 3H), 7.29 (br d, *J* = 8.6 Hz, 1H), 6.41 (br s, 1H).

4-Hydroxy-2-phenylquinoline-1-carboxylic acid ethyl ester (14i): Starting with *m*-methylcarboxylate aniline (**12i**) resulted in a mixture of several compounds. The crude mixture was subjected to the Mitsunobu reaction, as described below on the preformed tripeptide methyl ester.

***N*-(4-Hydroxy-2-phenylquinolin-7-yl)acetamide (14j):** Starting with *m*-acetamide aniline (**12j**) resulted in a mixture of several compounds. The mixture was subjected to the Mitsunobu reaction, as described below on the preformed tripeptide methyl ester.

7-Bromo-2-phenylquinolin-4-ol (14k): Starting with *m*-bromoaniline (**12k**) the title compound was obtained in 38% yield. ¹H NMR (DMSO-*d*₆): δ 8.01 (d, *J* = 8.5 Hz, 1H), 7.96 (d, *J* = 1.6 Hz, 1H), 7.84–7.79 (m, 2H), 7.61–7.56 (m, 3H), 7.48 (dd, *J* = 2.3, *J'* = 8.5 Hz, 1H), 6.36 (s, 1H).

7-Fluoro-2-phenylquinolin-4-ol (14l): Starting with *m*-fluoroaniline (**12l**) the title compound was obtained in 39% yield. ¹H NMR (DMSO-*d*₆): δ 8.14 (dd, *J* = 6.4, *J'* = 8.9 Hz, 1H), 7.87–7.78 (m, 2H), 7.63–7.55 (m, 3H), 7.48 (br d, *J* = 10.2 Hz, 1H), 7.20 (br t, *J* = 8.6 Hz, 1H), 6.34 (br s, 1H).

Preparation of Boc-4-*R*-(2-phenylquinolin-4-yl)oxyproline Derivatives 11a and 11b.²¹ The synthesis utilizes Boc-(4*S*)-*cis*-hydroxyproline methyl (**10a**) or benzyl (**10b**) ester and introduces the required substituted 2-phenyl-4-quinolin-4-yl moiety via a Mitsunobu reaction using diethyl azodicarboxylate and triphenylphosphine reagents.^{21,26} The resulting adduct was purified by flash column chromatography. The 4-*R*-aryloxyproline ester derivatives were hydrolyzed using aqueous lithium hydroxide in tetrahydrofuran. The resulting Boc protected amino acid was used in the next step without further purification.

Inhibitor Synthesis. All the inhibitors were prepared in solution by sequentially coupling (1*R*,2*S*)-1-amino-2-vinylcyclopropanecarboxylic acid methyl or ethyl ester to the previously prepared Boc-4-*R*-substituted-proline or appropriately protected Boc-4*S*-hydroxyproline using benzotriazol-1-yl-1,1,3,3-tetramethyluronium tetrafluoroborate (TBTU) or *N*-[(dimethylamino)-1*H*-1,2,3-triazolo[4,5-*b*]pyridin-1-ylmethylene]-*N*-methylmethanaminium hexafluorophosphate *N*-oxide (HATU) as the coupling agent. Removal of the *N*-Boc protective group was effected with 4 N HCl in dioxane to produce the dipeptide methyl or ethyl ester.

Synthesis of Compounds 15–23. Starting with the required dipeptide, the same reaction sequence described above was extended to Boc-valine (Boc-*tert*-leucine for **20** and **21**) and Boc-cyclohexylglycine. Subsequent introduction of the acetyl capping group (**15** to **20**) was done by treating the *N*-terminal amine with acetic anhydride. For compounds **22** and **23**, the required dipeptide was coupled with Boc-*tert*-leucine. After removal of the Boc-protecting group, the *N*-terminal amide was coupled using TBTU with the required carboxylic acid.

Synthesis of Compounds 24, 25, and 35–41. The required dipeptide was coupled with Boc-*tert*-leucine. For compounds **24**, **35**, and **36**, the Boc group was removed with HCl in dioxane and the resulting *N*-terminal amine was treated with either the cyclohexyl, the cyclopentyl, or the cyclobutyl chloroformate to produce cyclohexyl (**24**), cyclopentyl (**35**), and cyclobutyl (**36**) carbamate derivatives, respectively. Ureas **37**, **38**, and **39** were prepared by reacting the *N*-terminal tripeptide with cyclopentyl, cyclohexyl, and *tert*-butyl isocyanate, respectively. Urea **41** was obtained by treating the *N*-terminal tripeptide with triphosgene and reacting the resulting isocyanate with *N*-methyl-*N*-*tert*-butylamine. For the synthesis of compound **40**, the dipeptide was coupled to a preformed carbamate obtained by treating 1-*S*-hydroxy-3,3-dimethylbutyric acid benzyl ester with the cyclopentyl isocyanate and subsequent hydrogenation to the corresponding carboxylic acid.

Synthesis of Compounds 26–34. The synthesis was done by introducing the required aryloxy substituent on a preformed tripeptide methyl ester containing the *cis*-hydroxyproline

moiety. Mitsunobu reaction using diethyl azodicarboxylate and triphenylphosphine reagents²⁶ resulted in the required tripeptide methyl ester.

All the above-described compounds were subjected to hydrolysis of the methyl ester using aqueous LiOH in THF. The final compounds were purified by preparative HPLC using either a Whatman Partisil 10-ODS-3 column, 2.2 × 50 cm, or a YMC Combi-Prep ODS-AQ column, 50 × 20 mm, ID, S-5 μm, 120 Å, and a linear gradient program from 2 to 100% AcCN/water (0.06% TFA). Fractions were analyzed by analytical HPLC, and the pure fractions were combined, concentrated, frozen, and lyophilized to yield the desired compound as the trifluoroacetate salt.

Inhibitor Characterization and Purity. NMR spectra were recorded on a Bruker AMX400 (400 MHz for ¹H NMR) spectrometer and were referenced to TMS as an internal standard (0 ppm δ scale). Data are reported as follows: chemical shift (ppm), multiplicity (s = singlet, d = doublet, t = triplet, br = broad, m = multiplet), coupling constant (*J* – reported to the nearest 0.5 Hz), and integration. High-resolution mass spectra were obtained from a Micromass AutoSpec instrument using FAB as ionization mode with NBA as a matrix support. Inhibitor HPLC purity was measured by using an analytical C18 reversed phase column and two different eluting systems. Method A: 0.06% TFA in water–0.06% TFA in acetonitrile gradient (20%–100% acetonitrile over 30 min). Method B: 20 mM aqueous Na₂HPO₄ (pH 7.4)–acetonitrile gradient (20%–75% acetonitrile over 25 min).

Compound 15. ¹H NMR (DMSO-*d*₆): ca. 1:5 mixture of rotamers, only major rotamer described; δ 8.64 (s, 1H), 8.22–8.15 (m, 2H), 7.91–7.8 (m, 1H), 7.77–7.70 (m, 3H), 7.70–7.63 (m, 5H), 7.13 (bd, *J* = 8 Hz, 1H), 5.83–5.79 (m, 1H), 5.76–5.65 (m, 1H), 5.21 (dd, *J* = 1.6, *J'* = 17.5 Hz, 1H), 5.07 (dd, *J* = 1.3, *J'* = 10.5 Hz, 1H), 4.46 (dd, *J* = 8.3, *J'* = 6.7 Hz, 1H), 4.40 (dd, *J* = 7.6, *J'* = 9.5 Hz, 1H), 4.24 (d, *J* = 11.8 Hz, 1H), 4.17–4.09 (m, 1H), 4.06 (dd, *J* = 2.9, *J'* = 11.8 Hz, 1H), 3.81 (s, 3H), 2.34–2.19 (m, 1H), 2.14–1.98 (m, 2H), 1.83 (s, 3H), 1.79–1.73 (m, 1H), 1.61–1.39 (m, 8H), 1.28–1.22 (m, 1H), 1.16–0.97 (m, 4H), 0.91 (d, *J* = 6.7 Hz, 3H), 0.84 (d, *J* = 6.7 Hz, 3H). HRMS: found, 754.3816; calcd for C₄₂H₅₂N₅O₈, 754.3810. HPLC: (a) 97.6%; (b) 96.9%.

Compound 16. ¹H NMR (DMSO-*d*₆): ca. 1:5 mixture of rotamers, only major rotamer described; δ 8.62 (s, 1H), 8.20 (dd, *J* = 7.6, *J'* = 1.6 Hz, 2H), 8.1–8.04 (m, 1H), 7.82 (d, *J* = 8 Hz, 1H), 7.70 (s, 1H), 7.68–7.58 (m, 5H), 7.45 (d, *J* = 2.6 Hz, 1H), 5.80–5.73 (m, 1H), 5.73–5.64 (m, 1H), 5.21 (dd, *J* = 1.9, *J'* = 17.3 Hz, 1H), 5.07 (dd, *J* = 1.9, *J'* = 10.3 Hz, 1H), 4.45 (dd, *J* = 8.3, *J'* = 6.7 Hz, 1H), 4.39 (bd, *J* = 11.8 Hz, 1H), 4.29 (dd, *J* = 8, *J'* = 8 Hz, 1H), 4.16–4.06 (m, 2H), 3.93 (s, 3H), 2.62–2.53 (m, 1H), 2.35–2.26 (m, 1H), 2.07–1.90 (m, 2H), 1.81 (s, 3H), 1.70–1.61 (m, 1H), 1.61–1.35 (m, 7H), 1.28–1.22 (m, 1H), 1.13–0.97 (m, 4H), 0.94 (d, *J* = 6.7 Hz, 3H), 0.88 (d, *J* = 6.7 Hz, 3H). HRMS: found, 754.3806; calcd for C₄₂H₅₂N₅O₈, 754.3810. HPLC: (a) 98.3%; (b) 97.6%.

Compound 17. ¹H NMR (DMSO-*d*₆): ca. 1:5 mixture of rotamers, only major rotamer described; δ 8.60 (s, 1H), 8.18 (bd, *J* = 3.4 Hz, 3H), 8.00 (d, *J* = 7.8 Hz, 1H), 7.73 (d, *J* = 8.8 Hz, 1H), 7.67 (bs, 4H), 7.57–7.48 (m, 1H), 7.39–7.29 (m, 1H), 5.81–5.73 (m, 1H), 5.73–5.62 (m, 1H), 5.19 (dd, *J* = 1.9, *J'* = 17.3 Hz, 1H), 5.06 (dd, *J* = 1.9, *J'* = 10.3 Hz, 1H), 4.55–4.45 (m, 1H), 4.39–4.32 (m, 1H), 4.27–4.2 (m, 1H), 4.19–4.12 (m, 1H), 4.08–4.0 (m, 1H), 3.97 (s, 3H), 2.33–2.22 (m, 1H), 2.22–1.94 (m, 2H), 1.81 (s, 3H), 1.68–1.46 (m, 6H), 1.45–1.38 (m, 1H), 1.26–1.20 (m, 1H), 1.11–0.96 (m, 6H), 0.93 (d, *J* = 6.7 Hz, 3H), 0.89 (d, *J* = 6.7 Hz, 3H). HRMS: found, 754.3799; calcd for C₄₂H₅₂N₅O₈, 754.3810. HPLC: (a) 98.9%; (b) 95.1%.

Compound 18. ¹H NMR (DMSO-*d*₆): ca. 1:6 mixture of rotamers, only major rotamer described; δ 8.57 (s, 1H), 8.23 (d, *J* = 6.7 Hz, 2H), 7.97 (d, *J* = 8.3 Hz, 1H), 7.73 (d, *J* = 8.9 Hz, 1H), 7.70–7.63 (m, 2H), 7.62–7.52 (m, 3H), 7.47 (dd, *J* = 8, *J'* = 8 Hz, 1H), 7.32 (d, *J* = 7.6 Hz, 1H), 5.76–5.64 (m, 2H), 5.20 (dd, *J* = 1.9, *J'* = 17.3 Hz, 1H), 5.06 (dd, *J* = 1.9, *J'* = 10.3 Hz, 1H), 4.45–4.34 (m, 2H), 4.30 (dd, *J* = 8.3, *J'* = 8.3 Hz, 1H), 4.23–4.17 (m, 1H), 4.06 (dd, *J* = 3.5, *J'* = 11.8 Hz,

1H), 4.02 (s, 3H), 2.31–2.21 (m, 1H), 2.08 (s, 3H), 2.07–1.97 (m, 2H), 1.82 (s, 3H), 1.70–1.40 (m, 8H), 1.24 (dd, *J* = 4.9, *J'* = 9.2 Hz, 1H), 1.13–0.97 (m, 4H), 0.94 (d, *J* = 6.7 Hz, 3H), 0.88 (d, *J* = 6.7 Hz, 3H). HRMS: found, 754.3802; calcd for C₄₂H₅₂N₅O₈, 754.3810. HPLC: (a) 94.7%; (b) 94.7%.

Compound 19. ¹H NMR (DMSO-*d*₆): ca. 1:5 mixture of rotamers, only major rotamer described; δ 8.57 (s, 1H), 8.25 (d, *J* = 6.7 Hz, 2H), 7.94 (d, *J* = 8.3 Hz, 1H), 7.86 (d, *J* = 9.2 Hz, 1H), 7.74 (d, *J* = 8.9 Hz, 1H), 7.63–7.52 (m, 3H), 7.51 (s, 1H), 7.43 (d, *J* = 9.6 Hz, 1H), 5.76–5.65 (m, 2H), 5.20 (dd, *J* = 1.9, *J'* = 17.3 Hz, 1H), 5.06 (dd, *J* = 1.9, *J'* = 10.3 Hz, 1H), 4.42–4.35 (m, 1H), 4.29 (dd, *J* = 8.3, *J'* = 8.3 Hz, 1H), 4.22–4.15 (m, 1H), 4.08–4.01 (m, 2H), 4.04 (s, 3H), 3.97 (s, 3H), 2.62–2.52 (m, 1H), 2.31–2.20 (m, 1H), 2.08–1.97 (m, 2H), 1.82 (s, 3H), 1.69–1.38 (m, 8H), 1.24 (dd, *J* = 4.9, *J'* = 9.2 Hz, 1H), 1.13–0.97 (m, 4H), 0.94 (d, *J* = 6.7 Hz, 3H), 0.88 (d, *J* = 6.7 Hz, 3H). HRMS: found, 784.3903; calcd for C₄₃H₅₄N₅O₉, 784.3916. HPLC: (a) 96.8%; (b) 96.3%.

Compound 20. ¹H NMR (DMSO-*d*₆): ca. 1:6 mixture of rotamers, only major rotamer described; δ 8.60 (s, 1H), 8.23–8.12 (m, 3H), 7.78 (d, *J* = 8.6 Hz, 1H), 7.73–7.63 (m, 5H), 7.59–7.52 (bs, 1H), 7.34 (d, *J* = 8 Hz, 1H), 5.81–5.75 (m, 1H), 5.74–5.66 (m, 1H), 5.19 (dd, *J* = 1.9, *J'* = 17.3 Hz, 1H), 5.06 (dd, *J* = 1.9, *J'* = 10.3 Hz, 1H), 4.48–4.37 (m, 3H), 4.24 (dd, *J* = 8, *J'* = 8 Hz, 1H), 4.07–4.0 (m, 1H), 3.98 (s, 3H), 2.59–2.51 (m, 1H), 2.35–2.26 (m, 1H), 2.01 (dd, *J* = 8.8, *J'* = 17.3 Hz, 1H), 1.83 (s, 3H), 1.68–1.40 (m, 8H), 1.26 (dd, *J* = 4.9, *J'* = 9.2 Hz, 1H), 0.99 (s, 9H), 0.97–0.85 (m, 4H). HRMS: found, 768.3954; calcd for C₄₃H₅₄N₅O₈, 768.3967. HPLC: (a) 96.4%; (b) 95.7%.

Compound 21. ¹H NMR (DMSO-*d*₆): δ 8.64 (s, 1H), 8.36 (d, 1H, *J* = 8.6 Hz, 1H), 8.29–8.21 (m, 2H), 8.12–7.92 (m, 4H), 7.66–7.54 (m, 4H), 7.49 (bs, 1H), 7.23 (d, *J* = 8.9 Hz, 1H), 5.78–5.66 (m, 2H), 5.18 (dd, *J* = 1.6 Hz, *J'* = 17.2 Hz, 1H), 5.06 (dd, *J* = 1.6 Hz, *J'* = 10.5 Hz, 1H), 4.54 (d, *J* = 8.9 Hz, 1H), 4.42 (m, 1H), 4.28 (d, *J* = 12.4 Hz, 1H), 4.04 (dd, *J'* = 2.9 Hz, *J* = 11.8 Hz, 1H), 3.95 (s, 3H), 2.34–2.21 (m, 1H), 2.08–1.96 (m, 1H), 1.73–1.37 (m, 7H), 1.31–1.20 (m, 2H), 1.04 (s, 9H), 1.02–0.90 (m, 6H). HRMS: found, 726.3857; calcd for C₄₁H₅₂N₅O₇, 726.3861. HPLC: (a) 93.8%; (b) 86.5%.

Compound 22. ¹H NMR (DMSO-*d*₆): δ 8.59 (s, 1H), 8.25–8.12 (m, 3H), 7.72 (d, *J* = 8.6 Hz, 1H), 7.69–7.58 (m, 5H), 7.52 (bs, 1H), 7.21 (d, *J* = 9.2 Hz, 1H), 5.79–5.65 (m, 2H), 5.19 (dd, *J* = 1.4 Hz, *J'* = 17.0 Hz, 1H), 5.05 (dd, *J* = 1.9 Hz, *J'* = 10.2 Hz, 1H), 4.51–4.33 (m, 2H), 4.06–3.97 (m, 1H), 3.96 (s, 3H), 2.35–2.19 (m, 2H), 2.08–1.96 (m, 1H), 1.72–1.31 (m, 6H), 1.29–1.17 (m, 2H), 0.99 (s, 9H), 0.89 (d, *J* = 6.7 Hz, 3H), 0.97–0.71 (m, 7H). HRMS: found, 725.3902; calcd for C₄₂H₅₃N₄O₇, 725.3909. HPLC: (a) 98.6%; (b) 99.3%.

Compound 23. ¹H NMR (DMSO-*d*₆): δ 8.57 (s, 1H), 8.23–8.12 (m, 3H), 7.80 (d, *J* = 8.9 Hz, 1H), 7.75–7.62 (m, 5H), 7.60–7.53 (m, 1H), 7.30 (d, *J* = 8.3 Hz, 1H), 5.82–5.65 (m, 2H), 5.19 (dd, *J* = 1.6 Hz, *J'* = 17.2 Hz, 1H), 5.07 (dd, *J* = 1.9 Hz, *J'* = 10.5 Hz, 1H), 4.52–4.37 (m, 2H), 4.37 (d, *J* = 8.6 Hz, 1H), 4.05–3.98 (m, 1H), 3.97 (s, 3H), 2.65–2.53 (m, 1H), 2.37–2.25 (m, 1H), 2.08–1.89 (m, 2H), 1.75–1.38 (m, 9H), 1.30–1.22 (m, 1H), 1.16–1.01 (m, 2H), 0.96 (s, 9H), 0.86–0.71 (m, 2H). HRMS: found, 711.3750; calcd for C₄₁H₅₁N₄O₇, 711.3752. HPLC: (a) 97.4%; (b) 95.1%.

Compound 24. ¹H NMR (DMSO-*d*₆): δ 8.57 (s, 1H), 8.28–8.12 (m, 3H), 7.77–7.43 (m, 5H), 7.33–7.11 (m, 1H), 7.04 (d, *J* = 8.6 Hz, 1H), 5.82–5.63 (m, 2H), 5.19 (dd, *J* = 1.6 Hz, *J'* = 17.5 Hz, 1H), 5.06 (dd, *J* = 1.9 Hz, *J'* = 10.2 Hz, 1H), 4.52–4.39 (m, 2H), 4.14–4.04 (m, 1H), 3.96 (s, 3H), 2.64–2.43 (m, 2H), 2.35–2.25 (m, 1H), 2.08–1.97 (m, 1H), 1.73–1.43 (m, 7H), 1.36–1.06 (m, 6H), 0.96 (s, 9H). HRMS: found, 713.3554; calcd for C₄₀H₄₉N₄O₈, 713.3545. HPLC: (a) 97.4%; (b) 96.0%.

Compound 25. ¹H NMR (DMSO-*d*₆): δ 8.58 (s, 1H), 8.27–8.15 (m, 3H), 7.75–7.57 (m, 4H), 7.52 (bs, 1H), 7.21 (d, *J* = 7.6 Hz, 1H), 6.75 (d, *J* = 7.6 Hz, 1H), 5.81–5.65 (m, 2H), 5.18 (dd, *J* = 1.6 Hz, *J'* = 17.2 Hz, 1H), 5.06 (dd, *J* = 2.2 Hz, *J'* = 10.2 Hz, 1H), 4.54–4.40 (m, 2H), 4.04 (d, *J* = 8.3 Hz, 1H), 3.99–3.90 (m, 1H), 3.96 (s, 3H), 2.63–2.58 (m, 1H), 2.35–2.24 (m, 1H), 2.35–2.24 (m, 1H), 2.07–1.97 (m, 1H), 1.59–1.52 (m,

1H), 1.30–1.19 (m, 1H), 1.22 (s, 9H), 0.97 (s, 9H). HRMS: found, 687.3388; calcd for $C_8H_{47}N_4O_8$, 687.3388. HPLC: (a) 93.5%; (b) 94.4%.

Compound 26. 1H NMR (DMSO- d_6): δ 8.57 (s, 1H), 8.31–8.18 (m, 3H), 8.15–8.08 (m, 1H), 7.95–7.83 (m, 1H), 7.71 (s, 1H), 7.69–7.54 (m, 4H), 6.75 (d, J = 8.3 Hz, 1H), 5.82–5.66 (m, 2H), 5.18 (dd, J = 1.6 Hz, J' = 17.2 Hz, 1H), 5.06 (dd, J = 1.9 Hz, J' = 10.2 Hz, 1H), 4.56–4.39 (m, 2H), 4.07 (d, J = 8.6 Hz, 1H), 4.02–3.91 (m, 1H), 2.64–2.55 (m, 1H), 2.35–2.24 (m, 1H), 2.07–1.97 (m, 1H), 1.59–1.52 (m, 1H), 1.30–1.24 (m, 1H), 1.22 (s, 9H), 0.97 (s, 9H). HRMS: found, 657.3289; calcd for $C_37H_{45}N_4O_7$, 657.3283. HPLC: (a) 98.2%; (b) 95.1%.

Compound 27. 1H NMR (DMSO- d_6): ca. 1:15 mixture of rotamers, only major rotamer described; δ 8.59 (s, 1H), 8.22–8.16 (m, 3H), 7.71–7.62 (m, 4H), 7.52 (s, 1H), 7.21–7.16 (m, 1H), 6.74 (d, J = 8.6 Hz, 1H), 5.79–5.66 (m, 2H), 5.18 (d, J = 17.2, 1H), 5.05 (d, J = 10.5, 1H), 4.82 (h, J = 6.0, 1H), 4.51–4.43 (m, 1H), 4.02 (d, J = 8.3 Hz, 1H), 3.97–3.93 (m, 1H), 2.61–2.56 (m, 1H), 2.33–2.24 (m, 1H), 2.06–1.98 (m, 1H), 1.55 (dd, J = 4.9, J' = 7.8 Hz, 1H), 1.38 (d, J = 6.4 Hz, 6H), 1.29–1.25 (m, 1H), 1.20 (s, 9H), 0.97 (s, 9H). HRMS: found, 715.3698; calcd for $C_{40}H_{51}N_4O_8$, 715.3701. HPLC: (a) 92.3%; (b) 94.4%.

Compound 28. 1H NMR (DMSO- d_6): ca. 1:15 mixture of rotamers, only major rotamer described; δ 10.62 (s, 1H), 8.84 (s, 1H), 8.57 (s, 1H), 8.28–8.22 (m, 1H), 8.19–8.13 (m, 2H), 7.74–7.59 (m, 5H), 6.81 (d, J = 8.6 Hz, 1H), 5.82–5.66 (m, 2H), 5.18 (dd, J = 1.6, J' = 17.2 Hz, 1H), 5.05 (dd, J = 1.9, J' = 10.2 Hz, 1H), 4.51 (d, J = 11.2 Hz, 1H), 4.45–4.38 (m, 1H), 4.08–3.92 (m, 2H), 2.61–2.55 (m, 1H), 2.33–2.25 (m, 1H), 2.17 (s, 3H), 2.24–1.96 (m, 1H), 1.55 (dd, J = 5.1, J' = 7.9 Hz, 1H), 1.27 (s, 9H), 1.22–1.26 (m, 1H), 0.98 (s, 9H). HRMS: found, 714.3491; calcd for $C_{39}H_{48}N_5O_8$, 714.3497. HPLC: (a) 97.6%; (b) 95.3%.

Compound 29. 1H NMR (DMSO- d_6): ca. 1:8 mixture of rotamers, only major rotamer described; δ 8.59 (s, 1H), 8.23–8.19 (m, 2H), 8.13 (d, J = 9.0 Hz, 1H), 7.84 (s, 1H), 7.68–7.62 (m, 4H), 7.43 (d, J = 8.6 Hz, 1H), 6.74 (d, J = 8.0 Hz, 1H), 5.78–5.67 (m, 2H), 5.18 (dd, J = 1.6, J' = 17.1 Hz, 1H), 5.05 (dd, J = 1.9, J' = 10.5 Hz, 1H), 4.50–4.44 (m, 2H), 4.02 (d, J = 8.3, 1H), 3.93 (d, J = 9.9, 1H), 2.64 (s, 3H), 2.62–2.55 (m, 1H), 2.33–2.25 (m, 1H), 2.02 (dd, J = 8.6, J' = 17.5 Hz, 1H), 1.55 (dd, J = 5.1, J' = 7.9 Hz, 1H), 1.29–1.25 (m, 1H), 1.19 (s, 9H), 0.96 (s, 9H). HRMS: found, 703.3174; calcd for $C_{38}H_{47}N_4O_7S$, 703.3160. HPLC: (a) 95.2%; (b) 95.0%.

Compound 30. 1H NMR (DMSO- d_6): ca. 1:6 mixture of rotamers, only major rotamer described; δ 8.57 (s, 1H), 8.29–8.23 (m, 3H), 7.75 (dd, J = 2.2 Hz, J' = 10.2 Hz, 1H), 7.65–7.55 (m, 4H), 7.39–7.33 (m, 1H), 6.71 (d, J = 8.0 Hz, 1H), 5.76–5.66 (m, 2H), 5.18 (d, J = 17.2, 1H), 5.05 (d, J = 10.5, 1H), 4.48–4.40 (m, 2H), 4.08–3.92 (m, 2H), 2.59–2.52 (m, 1H), 2.33–2.23 (m, 1H), 2.06–1.98 (m, 1H), 1.55 (dd, J = 4.9, J' = 7.8 Hz, 1H), 1.29–1.25 (m, 1H), 1.21 (s, 9H), 0.97 (s, 9H). HRMS: found, 675.3180; calcd for $C_{37}H_{44}N_4O_7F$, 675.3189. HPLC: (a) 95.9%; (b) 93.8%.

Compound 31. 1H NMR (DMSO- d_6): ca. 1:12 mixture of rotamers, only major rotamer described; δ 8.58 (s, 1H), 8.29–8.25 (m, 2H), 8.23–8.19 (m, 1H), 8.09 (d, J = 8.9 Hz, 1H), 7.67 (s, 1H), 7.63–7.55 (m, 3H), 6.69 (d, J = 8.0 Hz, 1H), 5.76–5.66 (m, 2H), 5.22 (d, J = 15.6, 1H), 5.05 (d, J = 10.2, 1H), 4.48–4.39 (m, 2H), 4.02 (d, J = 8.6, 1H), 3.89–3.94 (m, 1H), 2.58–2.55 (m, 1H), 2.33–2.23 (m, 1H), 2.06–1.98 (m, 1H), 1.55 (dd, J = 4.9, J' = 7.8 Hz, 1H), 1.29–1.25 (m, 1H), 1.18 (s, 9H), 0.96 (s, 9H). HRMS: found, 735.2395; calcd for $C_{37}H_{44}N_4O_7Br$, 735.2388. HPLC: (a) 89.6%; (b) 94.1%.

Compound 32. 1H NMR (DMSO- d_6): ca. 1:10 mixture of rotamers, only major rotamer described; δ 8.61–8.56 (m, 2H), 8.33–8.27 (m, 3H), 7.97 (d, J = 8.3 Hz, 1H), 7.75 (s, 1H), 7.65–7.57 (m, 3H), 6.73 (d, J = 8.3 Hz, 1H), 5.79–5.66 (m, 2H), 5.18 (d, J = 17.2, 1H), 5.05 (d, J = 10.5, 1H), 4.49–4.43 (m, 2H), 4.06 (d, J = 8.3 Hz, 1H), 3.97–3.93 (m, 1H), 2.61–2.56 (m, 1H), 2.33–2.24 (m, 1H), 2.06–1.98 (m, 1H), 1.55 (dd, J = 4.9, J' = 7.8 Hz, 1H), 1.29–1.25 (m, 1H), 1.20 (s, 9H), 0.97 (s, 9H).

HRMS: found, 701.3178; calcd for $C_{38}H_{45}N_4O_9$, 701.3181. HPLC: (a) 94.7%; (b) 95.1%.

Compound 33. 1H NMR (DMSO- d_6): δ 8.60 (s, 1H), 8.35–8.32 (m, 4H), 7.77 (s, 1H), 7.68 (d, J = 8.2 Hz, 1H), 7.62–7.54 (m, 3H), 6.68 (d, J = 8.0 Hz, 1H), 5.79–5.68 (m, 2H), 5.19 (dd, J = 1.6, J' = 17.2 Hz, 1H), 5.05 (dd, J = 1.9, J' = 10.2 Hz, 1H), 4.49 (dd, J = 8.0, J' = 8.0, 1H), 4.42 (d, J = 12.1 Hz, 1H), 4.01 (d, J = 8.3 Hz, 2H), 2.58 (dd, J = 7.6, J' = 15.0 Hz, 1H), 2.33–2.23 (m, 1H), 2.03 (dd, J = 8.9, J' = 17.5 Hz, 1H), 1.56 (dd, J = 4.8, J' = 7.6 Hz, 1H), 1.28 (dd, J = 5.1, J' = 9.2 Hz, 1H), 1.11 (s, 9H), 0.96 (s, 9H). HRMS: found, 725.3160; calcd for $C_{38}H_{44}N_4O_7F_3$, 725.3157. HPLC: (a) 96.2%; (b) 93.9%.

Compound 34. 1H NMR (DMSO- d_6): δ 8.58 (s, 1H), 8.31–8.25 (m, 3H), 7.93 (s, 1H), 7.70 (s, 1H), 7.62–7.54 (m, 3H), 7.44 (d, J = 8.9 Hz, 1H), 6.71 (d, J = 8.0 Hz, 1H), 5.77–5.67 (m, 2H), 5.18 (d, J = 1.6, J' = 17.2 Hz, 1H), 5.06 (dd, J = 1.9, J' = 10.2 Hz, 1H), 4.49–4.43 (m, 2H), 4.03 (d, J = 8.3 Hz, 1H), 3.93 (d, J = 9.2 Hz, 1H), 2.57 (dd, J = 7.0, J' = 14.0 Hz, 1H), 2.33–2.21 (m, 1H), 2.02 (dd, J = 8.9, J' = 17.2 Hz, 1H), 1.56 (dd, J = 5.1, J' = 7.6 Hz, 1H), 1.27 (dd, J = 4.8, J' = 9.2 Hz, 1H), 1.15 (s, 9H), 0.96 (s, 9H). HRMS: found, 741.3101; calcd for $C_{38}H_{44}N_4O_8F_3$, 741.3106. HPLC: (a) 91.6%; (b) 95.9%.

Compound 35. 1H NMR (DMSO- d_6): δ 8.58 (s, 1H), 8.25–8.14 (m, 3H), 7.71–7.53 (m, 5H), 7.28–7.20 (m, 1H), 7.01 (d, J = 8.6 Hz, 1H), 5.80–5.66 (m, 2H), 5.19 (dd, J = 1.6, J' = 16.9 Hz, 1H), 5.06 (dd, J = 1.9, J' = 10.5 Hz, 1H), 4.60–4.52 (m, 1H), 4.47 (dd, J = 7.6, J' = 7.6 Hz, 1H), 4.07 (d, J = 8.6 Hz, 1H), 3.96 (s, 3H), 2.58 (dd, J = 6.0, J' = 13.3 Hz, 1H), 2.34–2.25 (m, 1H), 2.02 (dd, J = 8.3, J' = 17.2 Hz, 1H), 1.70–1.29 (m, 8H), 1.26 (dd, J = 5.1, J' = 9.5 Hz, 1H), 0.96 (s, 9H). HRMS: found, 699.3394; calcd for $C_{39}H_{47}N_4O_8$, 699.3388. HPLC: (a) 95.6%; (b) 96.1%.

Compound 36. 1H NMR (DMSO- d_6): ca. 1:6 mixture of rotamers, only major rotamer described; δ 8.57 (s, 1H), 8.28–8.14 (m, 3H), 7.74–7.44 (m, 5H), 7.28 (d, J = 7.3 Hz, 1H), 7.13 (d, J = 7.6 Hz, 1H), 5.84–5.66 (m, 2H), 5.19 (d, J = 17.2 Hz, 1H), 5.06 (dd, J = 1.9, J' = 12.1 Hz, 1H), 4.50–4.34 (m, 3H), 4.07–3.90 (m, 2H), 3.98 (s, 3H), 2.64–2.54 (m, 1H), 2.35–2.25 (m, 1H), 2.07–1.94 (m, 3H), 1.88–1.76 (m, 2H), 1.68–1.37 (m, 3H), 1.29–1.22 (m, 1H), 0.96 (s, 9H). HRMS: found, 685.3230; calcd for $C_{38}H_{45}N_4O_8$, 685.3232. HPLC: (a) 97.8%; (b) 96.6%.

Compound 37. 1H NMR (DMSO- d_6): δ 8.58 (s, 1H), 8.25 (d, J = 9.2 Hz, 1H), 8.21–8.14 (m, 2H), 7.73–7.53 (m, 5H), 7.27 (d, J = 9.2 Hz, 1H), 5.99–5.86 (m, 2H), 5.80–5.67 (m, 2H), 5.20 (dd, J = 1.6, J' = 17.2 Hz, 1H), 5.07 (dd, J = 1.9, J' = 10.2 Hz, 1H), 4.58 (d, J = 11.8 Hz, 1H), 4.44 (dd, J = 9.2, J' = 9.2 Hz, 1H), 4.15 (d, J = 8.6 Hz, 1H), 3.98 (s, 3H), 3.37–3.27 (m, 1H), 3.01 (bs, 1H), 2.68–2.55 (m, 1H), 2.36–2.26 (m, 1H), 2.03 (dd, J = 8.9, J' = 17.5 Hz, 1H), 1.78–1.38 (m, 10H), 1.30–0.99 (m, 13 H), 0.94 (s, 9H). HRMS: found, 712.3716; calcd for $C_{40}H_{50}N_5O_7$, 712.3705. HPLC: (a) 95.3%; (b) 95.6%.

Compound 38. 1H NMR (DMSO- d_6): ca. 1:6 mixture of rotamers, only major rotamer described; δ 8.58 (s, 1H), 8.35–8.10 (m, 3H), 7.75–7.60 (m, 4H), 7.60–7.45 (m, 1H), 7.25–7.15 (m, 1H), 5.99 (d, J = 6.4 Hz, 1H), 5.90 (d, J = 9.0 Hz, 1H), 5.80–5.65 (m, 2H), 5.19 (d, J = 17.0 Hz, 1H), 5.06 (d, J = 10.4 Hz, 1H), 4.56 (d, J = 11.6 Hz, 1H), 4.42 (dd, J = 8.8, J' = 8.8 Hz, 1H), 4.20–4.10 (m, 2H), 4.05–3.95 (m, 1H), 3.96 (s, 3H), 2.64–2.54 (m, 1H), 2.35–2.25 (m, 1H), 2.07–1.97 (m, 1H), 1.78–1.34 (m, 7H), 1.28–1.20 (m, 1H), 1.19–1.06 (m, 1H), 1.05–0.96 (m, 1H), 0.93 (s, 9H). HRMS: found, 698.3545; calcd for $C_{39}H_{48}N_5O_7$, 698.3548. HPLC: (a) 99.0%; (b) 95.8%.

Compound 39. 1H NMR (DMSO- d_6): δ 8.59 (s, 1H), 8.24 (d, J = 9.2 Hz, 1H), 8.20–8.13 (m, 2H), 7.71–7.51 (m, 6H), 7.23 (d, J = 9.2 Hz, 1H), 5.98–5.84 (m, 2H), 5.79–5.68 (m, 2H), 5.18 (d, J = 17.2 Hz, 1H), 5.06 (d, J = 10.2 Hz, 1H), 4.58 (d, J = 11.8 Hz, 1H), 4.42 (dd, J = 9.2, J' = 9.2 Hz, 1H), 4.12 (d, J = 6.7 Hz, 1H), 3.97 (s, 3H), 2.58 (dd, J = 7.0, J' = 13.3 Hz, 1H), 2.36–2.24 (m, 1H), 2.03 (dd, J = 8.9, J' = 17.4 Hz, 1H), 1.56 (dd, J = 5.1, J' = 7.6 Hz, 1H), 1.28–1.21 (m, 1H), 1.05 (s, 9H), 0.95 (s, 9H). HRMS: found, 686.3541; calcd for $C_{38}H_{48}N_5O_7$, 686.3548. HPLC: (a) 93.2%; (b) 89.1%.

Compound 40. 1H NMR (DMSO- d_6): δ 12.41 (bs, 1H), 8.56 (s, 1H), 8.50–8.04 (m, 1H), 8.23 (bs, 2H), 7.90–7.35 (m, 5H),

7.22 (d, $J = 6.9$ Hz, 1H), 5.80–5.61 (m, 1H), 5.17 (d, $J = 17.0$ Hz, 1H), 5.05 (d, $J = 10.4$ Hz, 1H), 4.71–4.61 (m, 1H), 4.55–4.37 (m, 2H), 3.94 (s, 3H), 3.86 (d, $J = 11.7$ Hz, 1H), 3.54–3.05 (m, under H₂O, 2H), 2.29–2.15 (m, 1H), 2.09–1.96 (m, 1H), 1.85–1.10 (m, 11H), 0.99 (s, 9H). HRMS: found, 699.3390; calcd for C₃₉H₄₇N₄O₈, 699.3388. HPLC: (a) 96.7%; (b) 90.1%.

Compound 41. ¹H NMR (DMSO-*d*₆): δ 8.58 (s, 1H), 8.24–8.14 (m, 3H), 7.72–7.47 (m, 6H), 7.23–7.15 (m, 1H), 5.78–5.66 (m, 2H), 5.51 (d, $J = 8.9$ Hz, 1H), 5.18 (d, $J = 16.9$ Hz, 1H), 5.06 (d, $J = 10.2$ Hz, 1H), 4.60–4.52 (m, 1H), 4.43 (dd, $J = 7.6$, $J' = 7.6$ Hz, 1H), 4.15 (d, $J = 8.6$ Hz, 1H), 3.96 (s, 3H), 2.75 (s, 3H), 2.62–2.52 (m, 1H), 2.34–2.24 (m, 1H), 2.02 (dd, $J = 8.9$, $J' = 17.5$ Hz, 1H), 1.55 (dd, $J = 5.1$, $J' = 7.6$ Hz, 1H), 1.29–1.22 (m, 1H), 1.13 (s, 9H), 0.99 (s, 9H). HRMS: found, 700.3698; calcd for C₃₉H₅₀N₅O₇, 700.3705. HPLC: (a) 96.0%.

Biological Assays. The values reported in both the enzymatic (IC₅₀) and the cell-based assay (EC₅₀) were determined using the protocols described in ref 22. The values reported are an average of at least four determinations.

Docking Protocol. The NS3 protease complex models of inhibitors **8** and **35** were obtained from energy minimization and molecular dynamics using Discover 95.0 and the CFF97 force field (Accelerlys Inc., San Diego, CA). The dynamics were performed without cross-terms and nonbonded cutoffs and with a dielectric constant of 1. First the compound (**8** or **35**) was built in a conformation that resembles the bound conformation previously determined for related analogues.^{21,30,31,36} The compound was then docked into the active site of the X-ray structure of the *apo* NS3 protease,⁹ using previously published crystal structures and complex models as guides for the initial step of docking.^{17,29–31,36} The inhibitor was appropriately oriented in order to allow its P1 carboxylate group to make H-bonds with the side chains of the catalytic triad residues His57 and Ser139, as well as with the backbone NH of the oxyanion hole residues Ser139 and Gly137, and in order to allow the formation of additional hydrogen bonds between the backbone NH and CO groups of the inhibitor P3 and the complementary backbone groups of the protein Ala157 residue. The bound inhibitor was then energy-minimized. The conformation of the protein and of the inhibitor P1 carboxylate were kept fixed during this first minimization step. This initial complex model was subsequently soaked in a 20 Å sphere of water. The NS3 protein and the water molecules were then divided into three zones and tethered to a different extent during the simulation: zone 1, 0–10 Å away from the center of mass of the inhibitor; zone 2, 10–15 Å away from the inhibitor; zone 3, >15 Å away from the inhibitor. The entire complex was first submitted to energy minimization and then to 1 ns of dynamics at 298 K following a 200 ps equilibration step. Zone 3 was kept fixed during this entire simulation, while zone 2 and zone 1 were tethered using quadratic force constants of 10 and 1 kcal/mol·Å², respectively, during the initial minimization step. These tethering force constants were then gradually reduced during the dynamic equilibration steps and were totally removed during the 1 ns dynamic run. In addition, the inhibitor P1 carboxylate was also tethered using a quadratic force constant of 1 kcal/mol·Å² during the initial steps. The bond lengths and water molecule angles were kept fixed during the entire dynamic simulation using rattle. At the end of the dynamics, the complex was further minimized (including cross-terms) to a final gradient of 0.1 kcal/mol·Å. The final NS3 protease complex models of inhibitors **8** and **35**, which resulted from these calculations, are shown in Figures 1 and 2, respectively (with omission of the water molecules for clarity).

Acknowledgment. We thank Diane Thibeault, Ewald Welchner, Dr. Lisette Lagacé, and Nathalie Dansereau for IC₅₀ and EC₅₀ determinations. Colette Boucher and Serge Valois are acknowledged for their excellent analytical support. We are grateful to Drs. Peter White and Michael Bös for critical reading of the manuscript. Finally we thank Drs. Paul Anderson,

Michael Cordingley and Daniel Lamarre for encouragement and support.

Supporting Information Available: 1D and 2D NMR (COSY, ROESY, HMQC, and HMBC) spectra of compound **38** with assignments. This material is available free of charge via the Internet at <http://pubs.acs.org>.

References

- Choo, Q.-L.; Kuo, G.; Weiner, A. J.; Overby, L. R.; Bradley, D. W.; Houghton, M. Isolation of a cDNA clone derived from a blood-borne non-A, non-B viral hepatitis genome. *Science* **1989**, *244*, 359.
- Hagedorn, C. H.; Rice, C. M. The hepatitis C virus. *Curr. Top. Microbiol. Immunol.* **2000**, *242*.
- Di Bisceglie, A. M. Hepatitis C. *Lancet* **1998**, *351*, 351–355.
- World Health Organization: Hepatitis C. Seroprevalence of hepatitis C virus (HCV) in a population sample. *Weekly Epidemiol. Rec.* **1996**, *71*, 346–349.
- Cornberg, M.; Wedemeyer, H.; Manns, M. P. Treatment of chronic hepatitis C with PEGylated interferon and ribavirin. *Curr. Gastroenterol. Rep.* **2002**, *4*, 23–30.
- Beaulieu, P. L.; Llinàs-Brunet, M. Therapies for Hepatitis C Infection: Targeting the Non-Structural Proteins of HCV. *Curr. Med. Chem.—Anti-Infective Agents* **2002**, *1*, 163–176.
- Walker, M. P.; Yao, N.; Hong, Z. Promising candidates for treatment of chronic hepatitis C. *Expert Opin. Investig. Drugs* **2003**, *12* (8), 1269–1280.
- De Francesco R.; Tomei, L.; Altamura, S.; Summa, V.; Migliaccio, G. Approaching a new era for hepatitis C virus therapy: Inhibitors of the NS3–4A serine protease and the NS5B RNA-dependent RNA polymerase. *Antiviral Res.* **2003**, *1807*, 1–16.
- Lamarre, D.; Anderson, P.; Bailey, M.; Beaulieu, P.; Bolger, G.; Bonneau, P.; Bös, M.; Cameron, D.; Cartier, M.; Cordingley, M.; Faucher, A.-M.; Goudreau, N.; Kawai, S.; Kukolj, G.; Lagacé, L.; LaPlante, S.; Narjes, H.; Poirier, M.-A.; Rancourt, J.; St-George, R.; Sentjens, R. E.; Simoneau, B.; Steinmann, G.; Thibeault, D.; Tsantrizos, Y. Weldon, A. M.; Yong, C.-L.; Llinàs-Brunet, M. Discovery of BLN 2061—An NS3 protease inhibitors with first antiviral proof-of-concept in humans infected with hepatitis C virus. *Nature* **2003**, *426*, 186–189. See also: Hinrichsen, H.; et al. First report on the antiviral efficacy of BLN2061, a novel oral serine protease inhibitor, in patients with chronic hepatitis C genotype 1. *Hepatology* **2002**, *36*, 297A, Abst. 866.
- Llinàs-Brunet, M.; Bailey, M.; Bolger, G.; Brochu, C.; Faucher, A.-M.; Ferland, J.-M.; Garneau, M.; Ghio, E.; Gorys, V.; Grand-Maitre, C.; Halmos, T.; Lapeyre-Paquette, N.; Liard, F.; Poirier, M.; Rhéaume, M.; Tsantrizos, Y. S.; Lamarre, D. Structure-activity study on a novel series of macrocyclic inhibitors of the Hepatitis C virus NS3 protease leading to the discovery of BLN2061. *J. Med. Chem.* **2004**, *44*, 1605–1608.
- Reed, K. E.; Rice, C. M. Overview of hepatitis C virus genome structure, polyprotein processing, and protein properties. *Curr. Top. Microbiol. Immunol.* **2000**, *242*, 55–84.
- Bartenschlager, R.; Lohmann, V. Replication of hepatitis C virus. *J. Gen. Virol.* **2000**, *81*, 1631–1648.
- Lesk, A. M.; Fordham, W. D.; Conservation and variability in the structure of serine proteinases of the chymotrypsin family. *J. Mol. Biol.* **1996**, *258*, 501–537.
- (a) De Francesco R.; Steinkühler, C. Structure and function of hepatitis C virus NS3–NS4A serine proteinase. *Hepatitis C Virus* **2000**, *242*, 149–169. (b) Steinkühler, C.; Koch, U.; Narjes, F.; Matassa, V. G. Hepatitis C virus serine protease inhibitors: Current progress and future challenges. *Curr. Med. Chem.* **2001**, *8*, 919–932.
- Kolykhalov, A. A.; Mihalik, K.; Feinstone, S. M.; Rice, C. M. Hepatitis C Virus-Encoded Enzymatic Activities and Conserved RNA Elements in the 3' Nontranslated Region Are Essential for Virus Replication In Vivo. *J. Virol.* **2000**, *74*, 2046.
- Llinàs-Brunet, M.; Bailey, M.; Fazal, G.; Goulet, S.; Halmos, T.; LaPlante, S.; Maurice, R.; Poirier, M.; Poupart, M.-A.; Thibeault, D.; Wernic, D.; Lamarre, D. Peptide-based inhibitors of the hepatitis C virus serine protease. *Bioorg. Med. Chem. Lett.* **1998**, *8*, 1713–1718.
- Steinkühler, C.; Biasiol, G.; Brunetti, M.; Urbani, A.; Koch, U.; Cortese, R.; Pessi, A.; De Francesco, R. Product inhibition of the hepatitis C virus NS3. *Biochemistry* **1998**, *37*, 8899–8905.
- Llinàs-Brunet, M.; Bailey, M.; Déaël, R.; Fazal, G.; Gorys, V.; Goulet, S.; Halmos, T.; Maurice, R.; Poirier, M.; Poupart, M.-A.; Rancourt, J.; Thibeault, D.; Wernic, D.; Lamarre, D. Studies on the C-terminal of hexapeptide inhibitors of the hepatitis C virus serine protease. *Bioorg. Med. Chem. Lett.* **1998**, *8*, 2719–2724.

- (19) Llinàs-Brunet, M.; Bailey, M.; Fazal, G.; Ghiro, E.; Gorys, V.; Goulet, S.; Halmos, T.; Maurice, R.; Poirier, M.; Poupart, M.-A.; Rancourt, J.; Thibeault, D.; Wernic, D.; Lamarre, D. Highly potent and selective peptide-based inhibitors of the hepatitis C virus serine protease: Towards smaller inhibitors. *Bioorg. Med. Chem. Lett.* **2000**, *10*, 2267–2270.
- (20) (a) Rancourt, J.; Cameron, D.; Gorys, V.; Lamarre, D.; Poirier, M.; Thibeault, D.; Llinàs-Brunet, M. Peptide-based inhibitors of the Hepatitis C Virus NS3 protease: Structure–Activity relationship at the C-terminal position. *J. Med. Chem.* **2004**, *47*, 2511–2422. (b) Boehringer-Ingelheim (Canada) Ltd. Hepatitis C inhibitor tripeptides. US Patent 6,323,180 B1 (2001).
- (21) Goudreau, N.; Cameron, D. R.; Bonneau, P.; Gorys, V.; Plouffe, C.; Poirier, M.; Lamarre, D.; Llinàs-Brunet, M. NMR Structural Characterization of Peptide Inhibitors Bound to the HCV NS3 Protease: Design of a New P2 Substituent. *J. Med. Chem.* **2004**, *47*, 123–132.
- (22) Pause, A.; Kukulj, G.; Bailey, M.; Brault, M.; Dô, F.; Halmos, T.; Lagacé, L.; Maurice, R.; Marquis, M.; McKercher, G.; Pellerin, C.; Pilote, L.; Thibeault, D.; Lamarre, D. An NS3 serine protease inhibitor abrogates replication of subgenomic hepatitis C virus RNA. *J. Biol. Chem.* **2003**, *278*, 20374–20380.
- (23) Lohmann, V.; Körner, F.; Koch, J. O.; Herian, U.; Theilmann, L.; Bartenschlager, R. Replication of Subgenomic Hepatitis C Virus RNAs in a Hepatoma Cell Line. *Science* **1999**, *285*, 110–113.
- (24) Lipinski, C. A.; Lombardo, F.; Domony, B. W.; Feeney, P. J. *Adv. Drug Delivery Rev.* **1997**, *23*, 3.
- (25) Poupart, M.-A.; Cameron, D. R.; Chabot, C.; Ghiro, E.; Goudreau, N.; Goulet, S.; Poirier, M.; Tsantrizos, Y. S.; Solid-phase synthesis of peptidomimetic inhibitors for the Hepatitis C virus NS3 protease. *J. Org. Chem.* **2001**, *66*, 4743–4751.
- (26) Mitsunobu, O. The Use of Diethyl Azodicarboxylate and Triphenylphosphine in Synthesis and Transformation of Natural Products. *Synthesis* **1981**, 1–28.
- (27) Giardina, G. A. M.; Sarau, H. M.; Farina, C.; Medhurst, A. D.; Grugni, M.; Raveglia, L. F.; Schmidt, D. B.; Rigolio, R.; Luttmann, M.; Vecchiotti, V.; Hay, D. W. P. Discovery of a novel class of selective non-peptide antagonists for the human neurokinin-3 receptor. 1. Identification of the 4-quinolinecarboxamide framework. *J. Med. Chem.* **1997**, *40*, 1794–1807.
- (28) Harrison, B. L.; Baron, B. M.; Cousino, D. M.; McDonald, I. A. 4-[(Carboxymethyl)oxy]- and 4-[(Carboxymethyl)amino]-5,7-dichloroquinoline-2-carboxylic acid: New antagonists of the Strychnine-insensitive glycine binding site on the *N*-methyl-D-aspartate receptor complex. *J. Med. Chem.* **1990**, *33*, 3130–3132.
- (29) Chun, M. W.; Olmstead, K. K.; Choi, Y. S.; Lee, C. O.; Lee, C.-K.; Kim, J. H.; Lee, J. Synthesis and biological activities of truncated acridone: Structure–activity relationship studies of cytotoxic 5-hydroxy-4-quinolone. *Bioorg. Med. Chem. Lett.* **1997**, *7*, 789–792.
- (30) LaPlante, S. R.; Cameron, D. R.; Aubry, N.; Lefebvre, S.; Kukulj, G.; Maurice, R.; Thibeault, D.; Lamarre, D.; Llinàs-Brunet, M. Solution structure of substrate-based ligands when bound to hepatitis C virus NS3 protease-domain. *J. Biol. Chem.* **1999**, *274*, 18618–18624.
- (31) LaPlante, S. R.; Aubry, N.; Bonneau, P. R.; Kukulj, G.; Lamarre, D.; Lefebvre, S.; Li, H.; Llinàs-Brunet, M.; Plouffe, C.; Cameron, D. R. NMR line-broadening and transferred NOESY as a medicinal chemistry tool for studying inhibitors of the Hepatitis C virus NS3 protease domain. *Bioorg. Med. Chem. Lett.* **2000**, *10*, 2271–2274.
- (32) Cicero, D. O.; Barbato, G.; Koch, U.; Ingallinella, P.; Bianchi, E.; Nardi, M.C.; Steinkühler, C.; Cortese, R.; Matassa, V. G.; De Francesco, R.; Pessi, A.; Bazzo, R. Structural characterization of the interactions of optimized product inhibitors with the N-terminal proteinase domain of the hepatitis C virus (HCV) NS3 protein by NMR and modeling studies. *J. Mol. Biol.* **1999**, *289*, 385–396.
- (33) Barbato, G.; Cicero, D. O.; Cordier, F.; Narjes, F.; Gerlach, B.; Sambucini, S.; Grzesiek, S.; Matassa, V. G.; De Francesco, R.; Bazzo, R. Inhibitor binding induces active site stabilization of the HCV NS3 protein serine protease domain. *EMBO J.* **2000**, *19*, 1195–1206.
- (34) Di Marco, S.; Rizzi, M.; Volpari, C.; Walsh, M. A.; Narjes, F.; Colarusso, S.; De Francesco, R.; Matassa, V. G.; Sollazzo, M. Inhibition of the hepatitis C virus NS3/4A protease: The crystal structures of two protease-inhibitor complexes. *J. Biol. Chem.* **2000**, *275*, 7152–7157.
- (35) Yao, N.; Reichet, P.; Taremi, S. S.; Prosser, W. W.; Weber, P. C. Molecular views of viral polyprotein processing revealed by the crystal structure of the hepatitis C virus bifunctional protease-helicase. *Structure* **1999**, *7*, 1353–1363.
- (36) Tsantrizos, Y. S.; Bolger, G.; Bonneau, P.; Cameron, D. R.; Goudreau, N.; Kukulj, G.; LaPlante, S. R.; Llinàs-Brunet, M.; Nar, H.; Lamarre, D. Macrocyclic inhibitors of the NS3 protease as potential therapeutic agents of hepatitis C virus infection. *Angew. Chem., Int. Ed.* **2003**, *42*, 1356–1360.
- (37) Kim, J. L.; Morgenstern, K. A.; Lin, C.; Fox, T.; Dwyer, M. D.; Landro, J. A.; Chambers, S. P.; Markland, W.; Lepre, C. A.; O'Malley, E. T.; Harbeson, S. L.; Rice, C. M.; Murcko, M. A.; Caron, P. R.; Thomson, J. A. Crystal structure of the hepatitis C virus NS3 protease domain complexed with a synthetic NS4A cofactor peptide. *Cell* **1996**, *87*, 343–355.
- (38) Narjes, F.; Koch, U.; Steinkühler, C. Recent developments in the discovery of hepatitis C virus serine protease inhibitors—Towards a new class of antiviral agents. *Expert Opin. Investig. Drugs* **2003**, *12* (2), 153–163 and reference therein.
- (39) Perni, R. B.; Britt, S. D.; Court, J. C.; Courtney, L. F.; Deininger, D. D.; Farmer, L. J.; Gates, C. A.; Harbeson, S. L.; Kim, J. L.; Landro, J. A.; Levin, R. B.; Luong, Y.-P.; O'Malley, E. T.; Pitlik, J.; Rao, B. G.; Schairer, W. C.; Thomson, J. A.; Tung, R. D.; Van Drie, J. H.; Wei, Y. Inhibitors of hepatitis C virus NS3–4A protease I. Noncharged tetrapeptide variants. *Bioorg. Med. Chem. Lett.* **2003**, *13*, 4059–4063.
- (40) LaPlante, S. R.; Aubry, N.; Déziel, R.; Ni, F.; Xu, P. Transferred ¹³C T₁ relaxation at natural isotopic abundance: A practical method for determining site-specific changes in ligand flexibility upon binding to a macromolecule. *J. Am. Chem. Soc.* **2000**, *122*, 12530–12535.
- (41) Slater, M. J.; Amphlett, E. M.; Andrews, D. M.; Bamborough, P.; Carey, S. J.; Johnson, M. R.; Jones, P. S.; Mills, G.; Parry, N. R.; Somers, D. O'N.; Stewart, A. J.; Skarzynski, T. Pyrrolidine-5,5-trans-lactams. 4. Incorporation of a P3/P4 urea leads to potent intracellular inhibitors of hepatitis C virus NS3/4A protease. *Org. Lett.* **2003**, *5* (24), 4627–4630.

JM0494523